Artículo en edición

Meteorologica

WIND RESOURCE ASSESSMENT IN THE RÍO NEGRO PROVINCE (PATAGONIA ARGENTINA) USING MERRA REANALYSIS

Tomás Manuel Guozden*[1,2], Emilio Bianchi[1], Andrés Solarte[1], Cristóbal Mulleady[3]

1 - Universidad Nacional de Río Negro

2 - Instituto Balseiro - Universidad Nacional de Cuyo

3 – Comisión Nacional de Energía Atómica

* Autor correspondiente: tguozden@unrn.edu.ar, Mitre 630 1C, Bariloche, Río Negro

Manuscrito recibido el 27/3/2017, aceptado el 13/09/2017

ABSTRACT

Argentinean Patagonia presents a large potential for wind energy generation. Currently, despite of several projects being developed, there is no installed wind power at Río Negro province. In the present paper, we perform an assessment of the wind energy resource in the province, using wind data derived from MERRA (Modern Era Retrospective Analysis for Research and Applications) reanalysis. We compared time series, histograms and wind roses between wind data derived from MERRA and wind data observed at several meteorological stations finding, in general, good agreement between them. We fitted the hourly wind data to a Weibull distribution for each grid point of the MERRA dataset, and mapped the mean annual wind speed and Weibull k factor. We then computed the capacity factors for different wind generators. We identified several different spots with optimal parameters and closeness to existing infrastructure (power lines and roads).

Keywords: Patagonia, wind energy, reanalysis

Artículo en edición

EVALUACIÓN DE RECURSOS EÓLICOS EN LA PROVINCIA DE RÍO NEGRO (PATAGONIA ARGENTINA) USANDO MERRA REANALYSIS

RESUMEN

La Patagonia Argentina presenta un gran potencial para la generación de energía eólica. Actualmente, y a pesar de que existen varios proyectos en desarrollo, no hay capacidad instalada en la provincia de Río Negro. En el presente trabajo se presenta una evaluación del recurso eólico en la provincia de Río Negro utilizando datos de viento derivados del reanálisis MERRA (Modern Era Retrospective Analysis for Research and Applications). Se compararon series de tiempo, histogramas y rosas de viento entre los datos derivados de MERRA y datos de viento observados en diferentes estaciones meteorológicas. Estas comparaciones mostraron, en líneas generales, buena correspondencia. Se ajustaron los datos horarios de viento a una distribución Weibull para cada punto de grilla de MERRA, y se mapearon los campos de velocidad media anual y el factor *k* de la distribución de Weibull. Luego se calcularon los factores de carga para diferentes tipos de aerogeneradores. Se pudieron identificar áreas con valores óptimos de velocidad media, factor *k* y factor de capacidad, y que además se encuentran cercanas a la infraestructura existente (líneas de transporte eléctrico y caminos.

Palabras clave: Patagonia, energía eólica, reanalisis

1. INTRODUCTION

The steppes of the Argentinean portion of Patagonia have a great potential for wind generation (Barros, 1983a, b; Laughton, 1990; Barros et al., 1997; Hoogwijk et al., 2004; Archer and Jacobson, 2005; De Vries et al., 2007; Lu et al., 2009). The symmetry of the zonal atmospheric circulation in the southern hemisphere and the depth of the circumpolar through (Peixoto and Oort, 1992; Kidson, 1988) determine that the wind speeds observed in this region are amongst the highest on earth (Palesse et al., 2000;

Pedro et al, 2006; Lu et al., 2009; Recalde, 2010). Estimated capacity factors for the Patagonian provinces oscillate between 25 and 50% (Guzowski and Recalde, 2008; Lu et al., 2009). Therefore, there is a general consensus that it would be feasible in the short term to increase the percentage of wind-generated electricity in the national grid (Recalde, 2010).

Despite this, Argentina has not significantly contributed yet to the global increase in the share of wind energy generation. The reason of this is that the energy matrix is primarily oriented towards the use of natural gas and fuel oil, and, so far, there has not been neither effective economic incentives nor proper legislation (Palesse et al, 2000, Guzowski and Recalde, 2008; Recalde, 2010). The previous tender (ENARSA Nº EE 01/2009 - GENREN), has not been successful mainly due to funding issues. Only 130 MW of the 754 MW originally awarded in the tender are currently operating. In particular, Río Negro is the only Patagonian province that does not have installed wind power up to date. In the last tender launched by the national government (Res MEM 071-2016 - Renovar) 6 wind energy generation projects were presented in the province of Río Negro for a total of 450 MW. Despite that only one project was awarded so far (50 MW, https://www.minem.gob.ar), this tender opens favorable perspectives for wind energy in the region.

Mapping the wind resource is fundamental for planning its exploitation properly. It allows identifying areas for potential developments and facilitates the design of resource evaluation at specific sites (Pedro et al., 2006). Several authors made important contributions in this way, quantifying the wind resource nationwide or for different provinces or regions. In most cases, these studies consisted in the integration of wind data measured in surface weather stations into meso-scale numeric models (Warchomicka et al., 2005; Pedro et al., 2006; Belmonte el al., 2006; Mattio, 2006; Aires et al., 2012; Samela et al., 2012).

Another way to quantify the wind resource is by using wind data derived from reanalysis (Lileo and Petrik, 2011; Jimenez et al., 2013). Reanalysis are constructed by data assimilation from synoptic weather stations, radiosondes, maritime buoys and satellites into global circulation models. There are currently several reanalysis available; for example the reanalysis of the National Center of Environmental Prediction (NCEP-

NCAR, Kalnay et al., 1996), the reanalysis of the European Centre for Medium-Range Weather Forecasts (ERA – Interim, Dee et al, 2011) and the Japanese reanalysis (JRA-55, Onogi et al., 2007). Lately, wind resource studies began to use the so called second generation reanalysis (MERRA, Rienecker et al., 2001, and CFSR, Saha et al., 2010), which improve temporal resolution (1 hour in the case of MERRA), horizontal (0.5° x 0.66°) and vertical with respect to first generation reanalysis.

The use of reanalysis data is accepted when the density observations is not sufficient to perform a regional climatic characterization (Bustos et al., 2016. Ferreli et al., 2016). Nevertheless, reanalysis data should be used with care since it does not represent micro-scale meteorological factors which do influence weather stations and significant differences between reanalysis data and observed data might arise (Rusticucci and Kouski, 2002;). Some authors (Zhao et al., 2007; Ferreli et al, 2016) propose the implementation of correction factors on the reanalysis data prior to its usage.

Despite this, the main advantages of the use of reanalysis data over the use of data measured in weather stations lie in that 1) weather stations might change its location or the environment in which they are placed might suffer changes, 2) Observational data might be affected by weathering and replacement of instruments (Otero et al., 2016) and 3) reanalysis offer wind estimations at several height levels (Cannon et al., 2015).

In the present study we evaluate the wind resource in the Río Negro province using wind data derived from MERRA reanalysis. In the first section, we evaluate the performance of MERRA in representing spatial and temporal patterns of the wind measured at 14 weather stations. In the second section we present wind resource maps and evaluate the quality of the resource.

2. DATA AND METHODOLOGY

Wind speed and wind direction data from 14 weather stations were compiled for the 2014-2015 period. The sources of this data are: the National Weather Service (SMN), the National Institute of Agricultural Research (INTA), and the provincial Department of Water (DPA). Figure 1 shows the location of the weather stations while the sources are specified in Table I. INTA and DPA use conventional automatic weather stations, in

which the sensors are usually placed at 2 meters height. SMN stations report data to the Global Climate Observation System (GCOS), and their wind stations are placed at 10 meters height. The temporal resolution of the data is 10 min. for INTA stations, hourly for SMN stations and daily for DPA stations respectively. Daily temporal resolution was used when comparing MERRA with DPA stations, and hourly temporal resolution was used when comparing MERRA with INTA and SMN stations. For this reason, hourly averages were computed from the original INTA 10 min. resolution series.

Figure 1.

Wind vector data from the Modern Era Retrospective-analysis for Research and Applications (MERRA, https://gmao.gsfc.nasa.gov/reanalysis/MERRA/) at 2, 10 and 50 m covering the 1979 – 2015 period was downloaded from https://disc.sci.gsfc.nasa.gov/daac-bin/FTPSubset.pl. MERRA was generated using the 5.2.0 version of the GEOS (Goddard Earth Observing System) atmospheric model, together with a data assimilation system. MERRA encompasses the 1979 – present period and its spatial resolution is 0.5º x 0.66º (Rienecker et al., 2011). Currently, MERRA is the only second-generation reanalysis being used in wind resource studies since the other reanalysis, CFSR, is no longer available since 2011. Several authors already highlighted the performance of MERRA in representing spatial and temporal patterns of wind variability (Hallgren et al., 2014; Cannon et al., 2015; Olauson and Bergkvist, 2015; Sharp et al., 2015).

Figure 2

Figure 3

Figure4

In order to validate MERRA wind data with measured data we computed, for each weather station, the correlation between observed wind speed at 2 meter height (10 meter height in the case of SMN stations) and wind speed from MERRA grid points. The direction of the wind was not considered in these correlations since only in the overall variation of wind speeds is relevant for wind energy generation. The correlation was computed for the 2014 – 2015 period. The distance between the location of the

station and the grid point at which the maximum correlation was observed is a measure of the spatial consistency between measured and MERRA – derived wind data. The spatial consistency between MERRA and winds derived from weather stations can also be observed in the three examples depicted in figure 5, which shows that the correlation between MERRA and the stations are maximum at pixel contiguous to the stations, and decay as the distance radius from the station increases.

Table I

Figure 5

The performance of the MERRA average wind speed field was compared to the average wind speed computed from observations by means of the residual metrics Bias (equation (1)), the Mean Absolute Error (MAE, equation (2)) and the Root Mean Squared Error (RMSE, equation (3))(Isaaks, 1989) between the observations at station locations and their respective nearest grid points. BIAS indicates whether a grid under or over estimates an observed variable, whereas MAE and RMSE are a measure of the absolute error. BIAS, MAE and RMSE statistics are defined as follows:

$$\text{BIAS} = \frac{1}{n}\sum_{i=1}^{n} r \qquad (1)$$

$$\text{MAE} = \frac{1}{n}\sum_{i=1}^{n} |r| \qquad (2)$$

$$\text{RMSE} = \sqrt{\frac{1}{n}\sum_{i=1}^{n} r^2} \qquad (3)$$

r = error = x' - x

n = *number of observational data* (4)

x' = closest grid point data

x = observational data

After comparing MERRA and observed wind data, we computed annual and seasonal mean wind speed and direction maps at 100 meters height, since this is the typical hub-

height of current wind generators. We use a power law relation (Archer and Jacobson, 2005) to extrapolate this value from 10 and 50 meters wind speed data, namely:

$$V(z) = V(z_{ref}) \left(\frac{Z}{z_{ref}}\right)^{\alpha} \quad (5)$$

where $V(z)$ is the wind speed elevation at elevation z, $V(z_{ref})$ is the wind speed at a reference elevation z_{ref} and α is known as the friction coefficient. We first compute α using wind speeds at 10 and 50 m, and then we use it to compute wind speeds at 100 m. Although this method has been widely used before (Mikhail, 1985; Lubitz, 2009; Kubik, 2013; Olauson, 2015; Genchi et al., 2016), assuming neutral stability when computing an hourly power law implies a significant aproximation due to changes in the atmospheric stability (Touma, 1977; Motta et al., 2005; Sen, 2012). Wind averages over long time periods, on the contrary, diminishes the incidence of atmospheric instabilities, since neutral stability conditions can be assumed (Anadranistakis et al., 2009). However, in our analysis, annual and seasonal extrapolated wind speed averages show minimal differences if they are computed from monthly or hourly values of 10 and 50 meters wind speeds (below 0.1% relative error). This is because is small and its variations are even smaller. For completeness, we show in figure 6 mean and deviation values for the friction coefficient .

Figure 6.

Then, in order to estimate the capacity factor at each grid point, we fit a distribution function to the wind speed histograms. Weibull distribution is the most accepted model to describe wind speed distributions (Spera, 1995; Patel, 1999; Ramos-Robles, 2005). The general expression of the Weibull distribution function is:

$$f(v) = \frac{k}{c}\left(\frac{v}{c}\right)^{k-1} e^{\frac{-v}{c}} \quad (6)$$

Where $f(v)$ is the probability function of wind speeds v, k is the shape parameter and c is the scale parameter, which is expressed in wind speed units. Both parameters describe

the curve that approximates the wind speed distribution (Weisser, 2003). *c* factor is associated with the mean wind speed while *k* expresses the kurtosis of the distribution. *k* is relevant since it is a measure of the intermittence of the energy dispatch of a wind farm. A wind speed distribution with high *k* (≈3) implies that wind speeds are concentrated around the mean value, and that the frequency of low and high wind speeds is low.

In order to adjust the Weibull distribution to the wind speed data derived from MERRA, hourly wind data were grouped in 0.5 m/s bins and a histogram was computed for each grid point. Then, a Weibull distribution function was fitted to the normalized histograms. This process was performed for the extrapolated values at 100 meters, but was also repeated for the 10 and 50 meters wind speed values. A remark should be done at this instance: the shape factor *k* for MERRA's wind speeds at 10 and 50 meters are very much the same, differing by less than a 1-2% relatively. And, as expected, the extrapolation performed does not alter the shape of the distribution: the shape factor for the extrapolated values, namely k_{100m}, is almost identical (below 1% relatively) to the shape factor found at 50 meters, namely k_{50m} . A good correspondence was found between the histograms and the Weibull distribution function, as it can be seen in the example in Figure 7a.

Finally we calculated the capacity factors at each grid point for power curves corresponding to three different International Electrotechnical Commission (IEC, see table II) classes. (Figure 7b). The different wind turbine generator classes are explained in table 3. Power curves relate wind speeds with the energy generated by a wind turbine generator. These power curves correspond to 3.45MW commercial turbines with diameters ranging between 110 and 130 meters and hub heights from 80 to 150 meters. Density variations due to temperature and surface elevation were neglected.

Figure 6.

For the computation of the capacity factors, the power curves of three 3.45 MW commercial wind generators (class IEC IA, class IEC IB – IIA and class IIB – IIIA)

were used. Capacity factors were computed by convolving the power curves with the Weibull distribution function for each grid point, as shown in equation 6:

$$LF_j = \frac{\sum_i POT(v_i) W_j(v_i) \Delta t}{P_{max}} \quad (7)$$

Where $POT(v)$ is the power curve and $W_j(v)$ is the Weibull distribution function for the grid point.

Table II

3. RESULTS

The maximum correlation coefficients between observed wind speed data at the weather stations and wind speed data from the MERRA grid are presented in Table Ia. Table Ia also shows the distance between each weather station and the grid point at which the maximum correlation was observed.

All correlation coefficients are significant at 99% confidence levels. The highest correlation is observed in Sierra Colorada ($r^2 = 0.74$, $p < 0.00001$), followed by Viedma ($r^2 = 0.42$, $p < 0.00001$) and Maquinchao ($r^2 = 0.4$, $p < 0.00001$). The distances between the stations and the maximum correlation grid point are below 100 km, with the exception of Valcheta (531 km) and Bariloche (155 km). The statistics bias, MAE and RMSE are shown in Table Ib. MERRA shows a tendency to overestimate wind speed (bias = 1.8 m/s). This overestimation determines that the values of the statistics MAE and RMSE are above 2 m/s, despite the high correlations between MERRA and the weather stations.

The regressions between wind speeds observed at INTA, DPA and SMN weather stations, and wind speed derived from MERRA is presented in Figure 8. The histograms of the different data subsets are also shown. All correlation coefficients are significant at $p < 0.00001$ (n = 33215, 93198 and 3085 for SMN, INTA and DPA stations, respectively). Example plots of the time series of MERRA wind speeds along with wind speeds measured in three weather stations are shown in figure 9

Figure 8.

Despite the significant correlations observed between MERRA and weather stations, measured wind speeds at 2 m height (INTA and DPA) show a higher frequency of weak wind and calms than MERRA and overall lower average speeds than winds measured at 10 m (SMN)(see Table I). This difference between station and MERRA data is probably a consequence of the location of the weather stations, which usually do not guarantee an obstacle free flow from all directions. INTA stations, for example, are often aimed to represent micro meteorological features inside a crop; while SMN stations, instead, are aimed to capture the general atmospheric motion. Both spatial and temporal resolution of the reanalysis also imposes a limit to its capacity to neither represent characteristic boundary layer wind variations nor small – scale wind – topography interactions. In this sense, it can be seen in Table I that MERRA consistently overestimates wind speeds at INTA and DPA stations, while it underestimates it at two of the three SMN stations (Bariloche and San Antonio).

Figure 9.

Annual and seasonal average wind speeds and direction maps for the 1979 – 2015 period are depicted in figure 10. Seasonal and annual average show similar spatial patterns. Mean wind speeds show their lowest values along the Andes Range (below 6 m/s approximately). The highest wind speeds (around 8 and 10 m/s) are seen towards the center of the province, coinciding with the highest sectors (from 900 masl. To 1100 masl. approximately, see Figure 1) of the Northern Patagonian Massif. Mean wind speeds decay towards north and northeast of the province, reaching values between 7 and 8 m/s. Wind speeds in the center of the province are lower during summer (8 m/s approximately). Previous works performed in Neuquen province reported annual wind speeds values ranging between 4 and 11 m/s throughout the province at 50 m. height (Pedro et al., 2006), and between 4 and 6.4 m/s at 10 m. height in three weather stations placed in the eastern part of the province (Palese et al., 2000).

Figure 10.

Each wind generatos class is assigned to a specific operation wind speed range (table II). The spatial variability in mean wind speeds described above determines different suitable areas for each wind class (figure 11). When applying class I power curve, the suitable area is located over the highest regions in the center of Río Negro (Figure 1), over the Northern Patagonian Massif, and over northern Chubut (Figure 11**(a)**). Capacity factors of around 60% are observed above the eastern and northern part of the Northern Patagonian Massif, nearby Los Menucos (40° 41´ S, 68° 07´ W).

Figure 11.

The suitable areas corresponding to the class I-II power curve (Figure 11**(b)**) lie over the western, central and eastern sectors of the province; and excludes areas where wind are either too weak or too strong over the northern and southern margins, and the western tip of the province over the Andes range. capacity factors range between 30% and 40% in the western sector of the province, between 50% and 60% in the center, and between 40% and 50% in the eastern sector of the province. For the class II-II power curve (Figure 11**(c)**), the suitable areas lie over the northwestern sector, and over the Andes range east of the province. For this class, capacity factors range between 30% and 50% approximately. Lu et al. (2009) reported similar capacity factors over northern Patagonia. In their study, capacity factors range between 35 to over 50% trhoughout the region, and the distribution shows a north – south gradient; with higher capacity factors over souther Patagonia and decreasing values northward.

The shape parameter (*k*) of the Weibull distribution (Figure 11**(d)**) ranges between 2.3 and 2.8, and shows its higher values (above 2.8) towards the eastern and northeastern sectors of the province. This parameter also shows local maximums in the extra-Andean high regions, namely the Northern Patagonian Massif. The values of *k* over the eastern part of Neuquen are coincident with values found in the previous analysis of Palesse et al. (2000). They reported values ranging from 1.5 to 2 in three weather stations.

4. CONCLUSIONS

MERRA´s second generation reanalysis is a robust tool to study the wind resource variability on a regional scale. Even though its spatial resolution (1/2º by 2/3º) sets a limit to its capacity to characterize the wind at a site scale, its temporal resolution (1 hour) and the length of the time series (37 years) make MERRA a useful tool to study wind variability over several time scales.

Wind speed data derived from MERRA show consistency with wind speed data from weather stations. Regressions between MERRA and observed wind speeds show significant correlation coefficients. MERRA, however, shows a tendency to overestimate wind speeds, in particular during low speed conditions. But on the other hand local features of the environment in which the weather stations are placed, such as slope, topography, closeness of buildings or vegetation, or surface rugosity, might alter the measurements. The spatial scale of the reanalysis and the physical phenomena represented by the general circulation model might also alter the comparisons between measured wind speeds and reanalysis derived wind speeds. For example, wind variations related to the boundary layer occur at a much finer resolution than that of MERRA. In addition, MERRA wind speed data are created by the assimilation of observational data from different sources into a general circulation model, so the errors involved in those processes might affect further analysis.

In the present work we present an analysis of the wind resource for the Río Negro province. Even though previous works have characterized the wind resource for different Argentinean provinces or regions (Palesse et al., 2000; Mattio, 2006; Recalde, 2010, Genchi et al., 2016), Río Negro lacked a detailed study of its wind resource. We identified zones where the wind resource shows favorable features for exploitation. For example, above the Northern Patagonian Massif (between 68º and 69º W, and between 40º and 41º S approximately) wind speeds at 100 m height range between 8 and 10 m/s, Weibull shape factors are above 2.8 and capacity factors reach about 50% and 60% for class I and II power curves respectively. Capacity factors reported in this study are

coincident with those found by the previous analysis of Lu et al. (2009) over northern Patagonia.

The consistency between observed and MERRA wind speeds, and the length (37 years) of the time series make this reanalysis an attractive tool for studying the temporal variability and tendencies of the wind resource, so too its response to large scale clime drivers, such as El Niño/Southern Oscillation.

Acknowledgments: This work was supported by 1) Agencia Nacional de Promoción Científica y Tecnológica, 2) Universidad Nacional de Río Negro. Ángel Muñoz and Martín Nini provided additional climate data. Diego Padilla and Martín Ureta provided information about power curves.

5. BIBLIOGRAPHY

Aires, M., De Bortoli, M. E., Frigerio, E., and Roko, S. R. 2015. Estimación de potencial eólico de la provincia de Misiones.

Anadranistakis, M., Kerkides, P., Liakatas, A., Alexandris, S., and Poulovasilis, A. 1999: How significant is the usual assumption of neutral stability in evapotranspiration estimating models?. *Meteorological Applications*, *6*(2), 155-158.

Archer, C. L., and Jacobson, M. Z. 2005: Evaluation of global wind power. *Journal of Geophysical Research: Atmospheres*, *110*(D12).

Bañuelos, F., Camacho, C., Serrano, J., and Muciño, D. 2008: Análisis y validación de Metodología usada para la obtención de perfiles de velocidad de viento. *Instituto de Ingeniería de la Universidad Nacional Autónoma de México*.

Barros, **V. 1983a**: Evaluación del potencial eólico en la Patagonia. *Meteorologica, XIV*, *1*, 473-484.

Barros, V. 1983b: *Atlas del potencial eólico de la Patagonia*. Secretaría de Estado de Ciencia y Tecnología-Consejo Nacional de Investigaciones Científicas y Técnicas-Centro Nacional Patagónico.

Barros, V., Camilloni, I., Frumento, O., and Rivero, M. 1997: Estudio del potencial eólico en la República Argentina. *Programa de Abastecimiento Eléctrico a la Población Rural Dispersa*.

Belmonte, S., de Monrós, J. T., Franco, J., Núñez, V., Manrique, S., and Mattio, H. 2006. Mapeo eólico del Valle de Lerma (Salta–Argentina). *Revista AVEREMA (Avances en Energías Renovables y Medio Ambiente) V*, *10*(2006), 06-23.

Bustos, M. L., Ferrelli, F., Cisneros, M. A. H., Piccolo, M. C., and Gil, V. 2016: Estudio preliminar del ajuste entre datos meteorológicos in situ y del Reanálisis (NCEP/NCAR) en distintos ambientes de la provincia de Buenos Aires, Argentina. *Estudios Geográficos*, *77*(280), 335-343.

Camblong, D. 2003: Minimización de impacto de las perturbaciones deorigen eólico en la generación por aeroturbinas de velocidad variable. Tesis doctoral. España: Mondragón Unibertsitatea; 2003

Cannon, D. J., Brayshaw, D. J., Methven, J., Coker, P. J., and Lenaghan, D. 2015. Using reanalysis data to quantify extreme wind power generation statistics: a 33 year case study in Great Britain. *Renewable Energy*, *75*, 767-778.

De Vries, B. J., Van Vuuren, D. P., and Hoogwijk, M. M. 2007: Renewable energy sources: Their global potential for the first-half of the 21st century at a global level: An integrated approach. *Energy policy*, *35*(4), 2590-2610.

Dee, D. P., Uppala, S. M., Simmons, A. J., Berrisford, P., Poli, P., Kobayashi, S., and Bechtold, P. 2011. The ERA-Interim reanalysis: Configuration and performance of the data assimilation system. *Quarterly Journal of the royal meteorological society*, *137*(656), 553-597.

Ferrelli, F., Bustos, M. L., Piccolo, M. C., Cisneros, M. A. H., and Perillo, G. M. E. 2016: Downscaling de variables climáticas a partir del reanálisis NCEP/NCAR en el sudoeste de la provincia de Buenos Aires (Argentina). *Papeles de Geografía*, (62).

Genchi, S. A., Vitale, A. J., Piccolo, M. C., and Perillo, G. M. 2016. Wind energy potential assessment and techno-economic performance of wind turbines in coastal sites of Buenos Aires province, Argentina. *International Journal of Green Energy*, *13*(4), 352-365.

Guzowski, C., and Recalde, M. 2008. Renewable energy in Argentina: Energy policy analysis and perspectives. *International Journal of Hydrogen Energy*, *33*(13), 3592-3595.

Hallgren, W., Gunturu, U. B., and Schlosser, A. 2014: The potential wind power resource in australia: a new perspective. *PloS one*, *9*(7), e99608.

Hoogwijk, M., de Vries, B., and Turkenburg, W. 2004: Assessment of the global and regional geographical, technical and economic potential of onshore wind energy. *Energy Economics*, *26*(5), 889-919.

Isaaks, E. H. 1989: Applied geostatistics (No. 551.72 I86). Oxford University Press.

Jimenez, B., Moennich, K., Oldenburg, D. E. W. I., Rey, J., Spain, D. E. W. I., and Durante, F. 2013. Use of different globally available long-term data sets and its influence on expected wind farm energy yields.

Kalnay, E., Kanamitsu, M., Kistler, R., Collins, W., Deaven, D., Gandin, L., and Zhu, Y. 1996. The NCEP/NCAR 40-year reanalysis project. *Bulletin of the American meteorological Society*, *77*(3), 437-471.

Kidson, J. W. 1988: Indices of the Southern Hemisphere zonal wind. *Journal of Climate*, *1*(2), 183-194.

Kubik, M. L., Brayshaw, D. J., Coker, P. J., and Barlow, J. F. 2013: Exploring the role of reanalysis data in simulating regional wind generation variability over Northern Ireland. *Renewable energy*, *57*, 558-561.

Laughton, M. A. (Ed.). 1990: Renewable Energy Sources*: Watt Committee: report number 22* (Vol. 22). CRC Press.

Liléo, S., and Petrik, O. 2011. Investigation on the use of NCEP/NCAR, MERRA and NCEP/CFSR reanalysis data in wind resource analysis. *Sigma. EWEC*, *1*(2).

Lu, X., McElroy, M. B., and Kiviluoma, J. 2009: Global potential for wind-generated electricity. *Proceedings of the National Academy of Sciences*, *106*(27), 10933-10938.

Lubitz, W. D. 2009: Power law extrapolation of wind measurements for predicting wind energy production. *Wind Engineering*, *33*(3), 259-271.

Mattio, H. F. 2006. SIG Eolico/Sistema de Información Geográfico-Mapa Eolico Nacional v2. 3.0 l.

Mikhail, A. S. 1985: Height extrapolation of wind data. *Journal of solar energy engineering*, *107*(1), 10-14.

Motta, M., Barthelmie, R. J., and Vølund, P. 2005: The influence of non-logarithmic wind speed profiles on potential power output at Danish offshore sites. *Wind Energy*, *8*(2), 219-236.

Olauson, J., and Bergkvist, M. 2015: Modelling the Swedish wind power production using MERRA reanalysis data. *Renewable Energy*, *76*, 717-725.

Onogi, K., Tsutsui, J., Koide, H., Sakamoto, M., Kobayashi, S., Hatsushika, H., and Kadokura, S. 2007. The JRA-25 reanalysis. *Journal of the Meteorological Society of Japan. Ser. II*, *85*(3), 369-432.

Otero, F., Cerne, B., and Campetella, C. 2016. Estudio preliminar de la velocidad del viento en San Julián en referencia a la generación de energía eólica. *Meteorológica*.

Palese, C., Lässig, J. L., Cogliati, M. G., and Bastanski, M. A. 2000: Wind regime and wind power in North Patagonia, Argentina. *Wind Engineering*, *24*(5), 361-377.

Patel, M.R. 1999: Wind and Solar Power Systems, New York: CRC Press LLC, 351 pp.

Pedro, G., Mattio, H., Palese, C., Warchomicka, N., and Lassig, J. 2006: Recurso eólico de la provincia del Neuquén. *Avances en Energías Renovables y Medio Ambiente*, *10*, 15-21.

Peixoto, J. P., and Oort, A. H. 1992: Physics of Climate, 520 pp. *Am. Inst. of Phys., New York*.

Ramos-Robles, C. A., and Irizarry-Rivera, A. A. 2005: Economical effects of the Weibull parameter estimation on wind energy projects. In *Proceedings of the 37th Annual North American Power Symposium, 2005.* (pp. 597-602). IEEE.

Recalde, M. 2010: Wind power in Argentina: Policy instruments and economic feasibility. *international journal of hydrogen energy*, *35*(11), 5908-5913.

Rienecker MM, Suarez MJ, Gelaro R, Todling R, Bacmeister J, Liu E, et al. 2011: MERRA - NASA's modern-era retrospective analysis for research and applications. *Journal of Climate,* 24, 3624-48.

Rusticucci M. M. and Kousky V. E. 2002: American Meterological Society. "A comparative study of maximum and minimum temperatures over Argentina: NCEP-NCAR Reanalysis versus station data", vol. 15, p. 2089-2101

Saha, S., Moorthi, S., Pan, H. L., Wu, X., Wang, J., Nadiga, S., and Liu, H. 2010. The NCEP climate forecast system reanalysis. *Bulletin of the American Meteorological Society*, *91*(8), 1015-1057.

Samela, A. M., Bahamonde, P. J., Calafiore, C. A., Bonfili, O. A., Queipul, J. A., García, D. H., and Rojas, C. 2012. Determinación de parámetros de vientos en el Sur de la provincia de Santa Cruz.

Şen, Z., Altunkaynak, A., and Erdik, T. 2012: Wind velocity vertical extrapolation by extended power law. *Advances in Meteorology*, *2012*.

Sharp, E., Dodds, P., Barrett, M., and Spataru, C. 2015: Evaluating the accuracy of CFSR reanalysis hourly wind speed forecasts for the UK, using in situ measurements and geographical information. *Renewable Energy*, *77*, 527-538.

Spera DA. 1995: Wind Turbine Technology. Fundamental Concepts of Wind Turbine Engineering. *The American Society of Mechanical Engineers*: New York, 638 pp.

Touma, J. S. 1977: Dependence of the wind profile power law on stability for various locations. *Journal of the Air Pollution Control Association*, *27*(9), 863-866.

Warchomicka, N., Palese, C., Pedro, G., Mattio, H., amd Lassig, J. 2005. Evaluación del recurso eólico del Departamento Confluencia de la Provincia del Neuquén. *Avances en Energías Renovables y Medio Ambiente*, *9*(6), 39-44.

Weisser, D. 2003: A wind energy analysis of Grenada: an estimation using the 'Weibull'density function. *Renewable energy*, *28*(11),

Zhao T., Guo W. and Fu C. **2007:** Journal of Climate. "Calibrating and evaluating reanalysis
surface temperature error by topographic correction", vol. 21, p. 1440-1446.

Figures

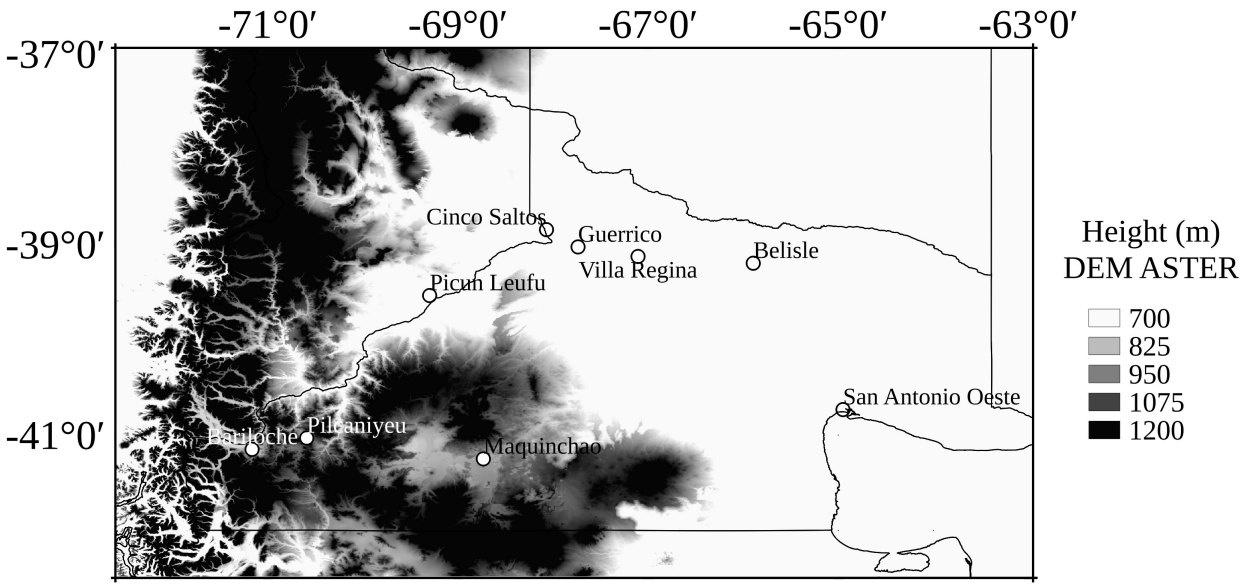

Figure 1: Location of weather stations and terrain elevation derived from ASTER Digital Elevation Model.

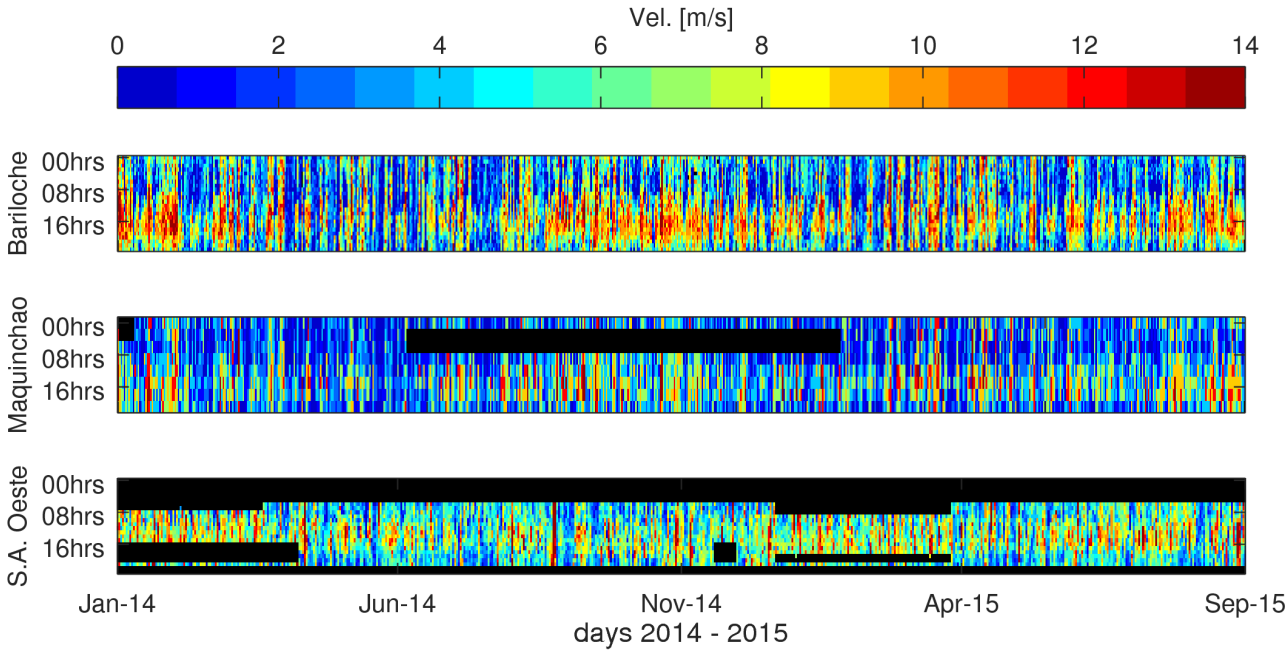

Figure 2. Timeseries of SMN stations. Blanked spaces denote missing data.

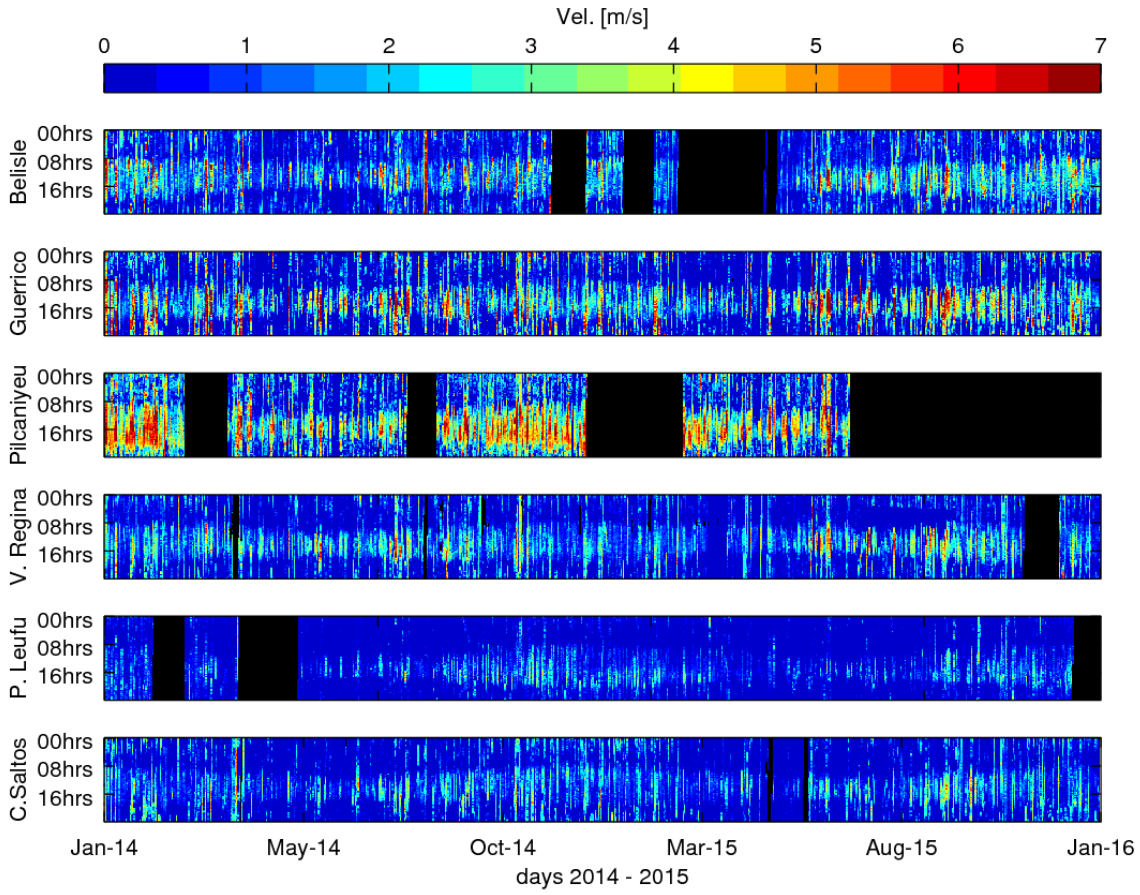

Figure 3.Timeseries of INTA stations. Blanked spaces denote missing data.

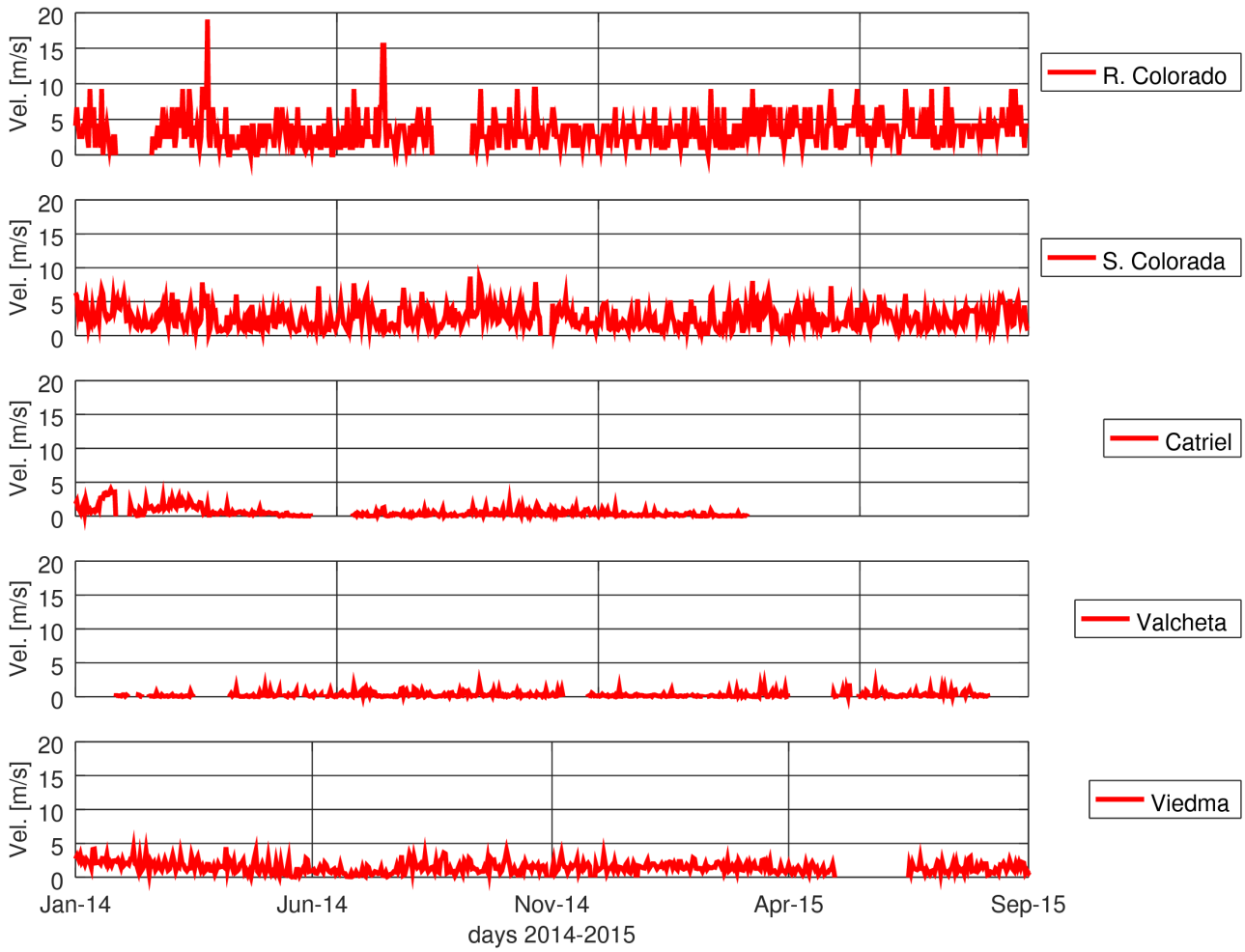

Figure 4. Timeseries of DPA stations.

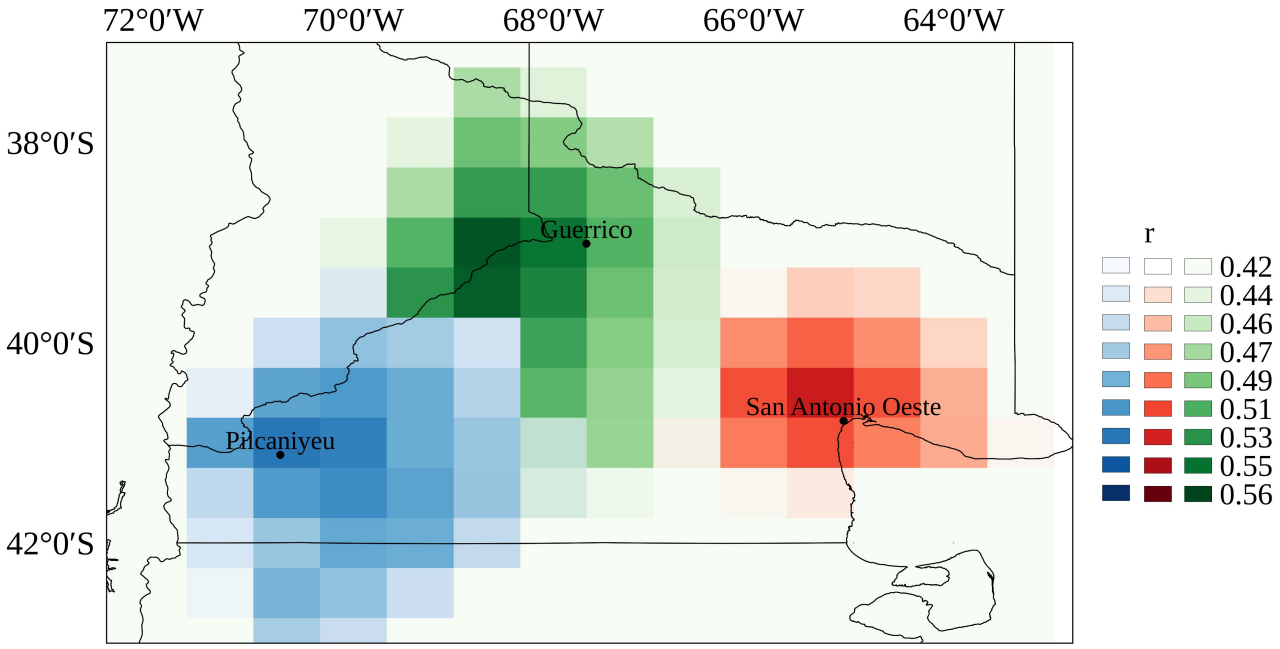

Figure 5. Spatial correlation patterns between wind speeds at Pilcaniyeu, San Antonio Oeste and Guerrico stations, and MERRA wind speeds.

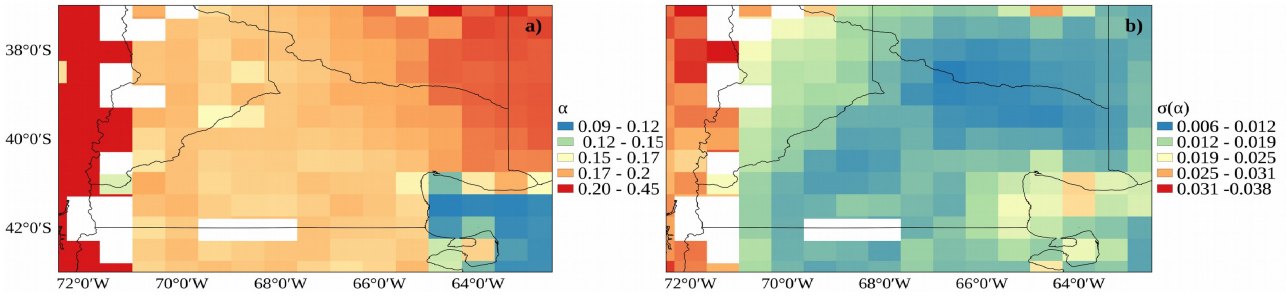

Figure 6: mean values (a) and deviations (b) for alpha. Terrain elevations above 1400 masl. were masked.

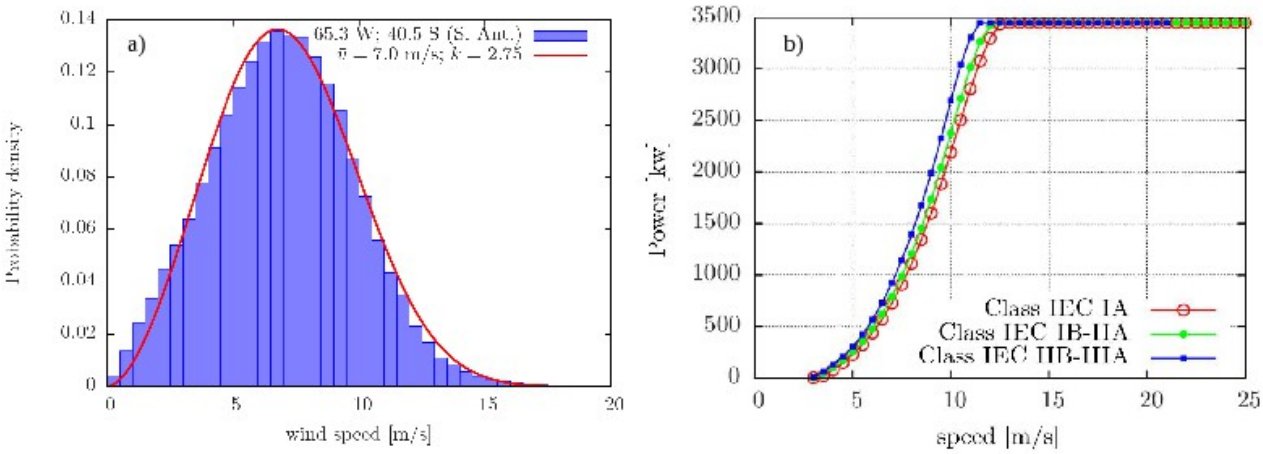

Figure 7: Example of a Weibull distribution function fitted to wind speed data at a MERRA grid point close to the San Antonio Oeste weather station (a). Power curves of the class I wind, class I and II, and class II and III wind generators (b)

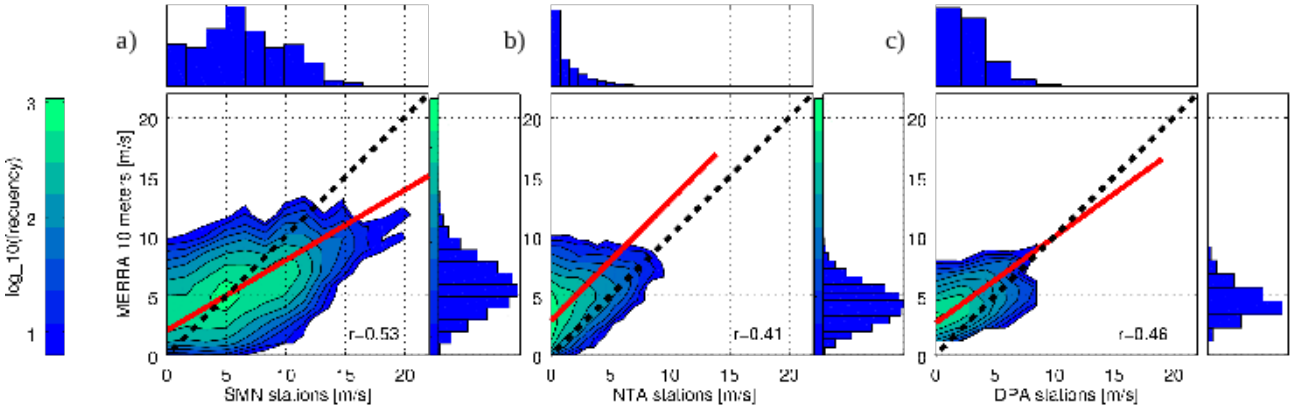

Figure 8: Regression (red lines) and histograms between hourly wind speeds averaged at SMN weather stations, and hourly 10 m. wind speeds derived from MERRA (a); hourly wind speeds averaged at INTA weather stations and 2 m. hourly wind speeds derived from MERRA (b), and daily wind speeds averaged at DPA weather stations and 2 m. daily wind speeds derived from MERRA. The dashed solid line indicates a 1:1 agreement, whereas the red line shows a linear least squares fit to the data.

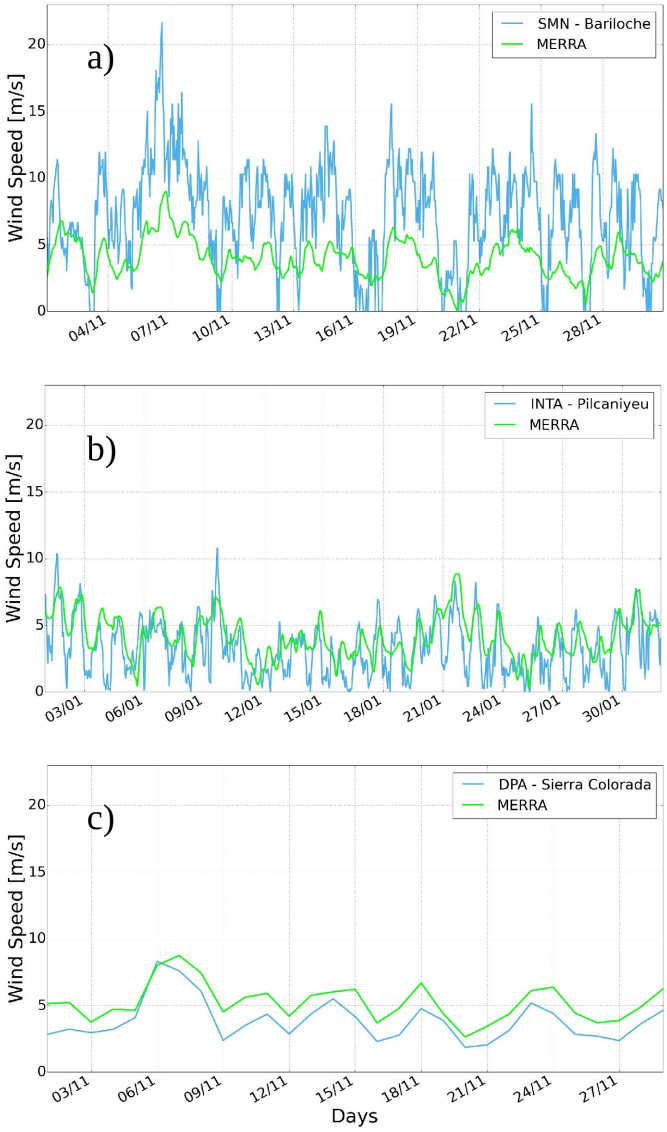

Figure 9: Time series of measured wind speed (blue lines) and MERRA wind speeds (green lines) at Bariloche (a), Pilcaniyeu (b) and Sierra Colorada (c) weather stations.

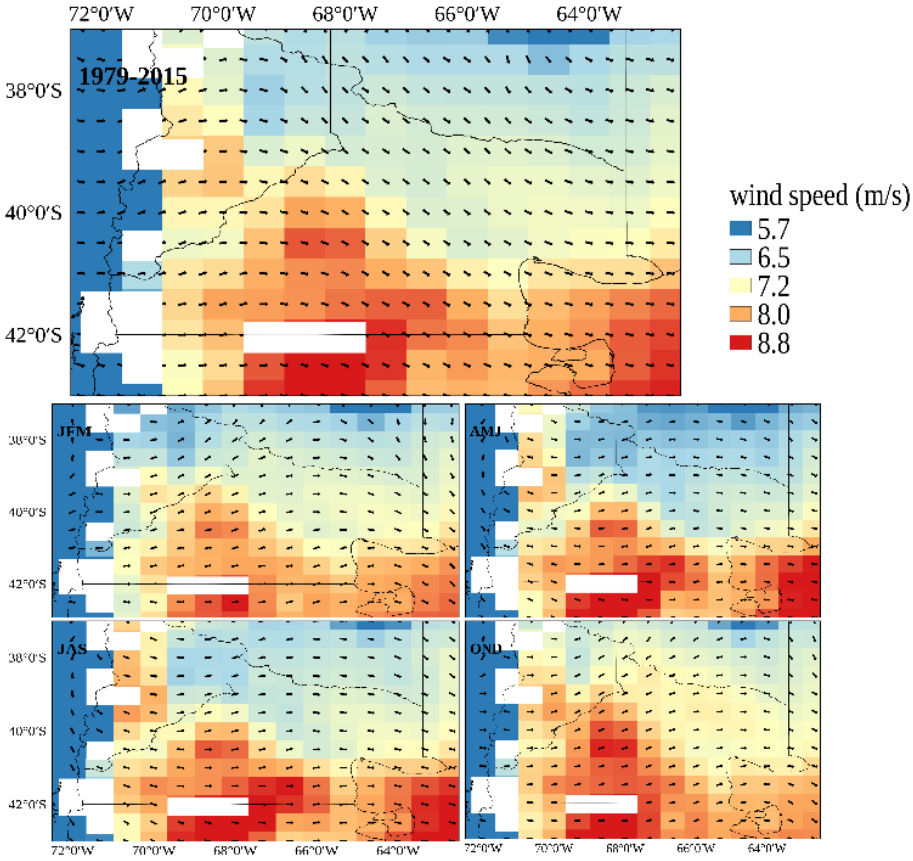

Figure 10: Mean annual and seasonal wind speed extrapolated at 100 m height derived from MERRA in the 1979 – 2015 period. Terrain elevations above 1400 masl. were masked.

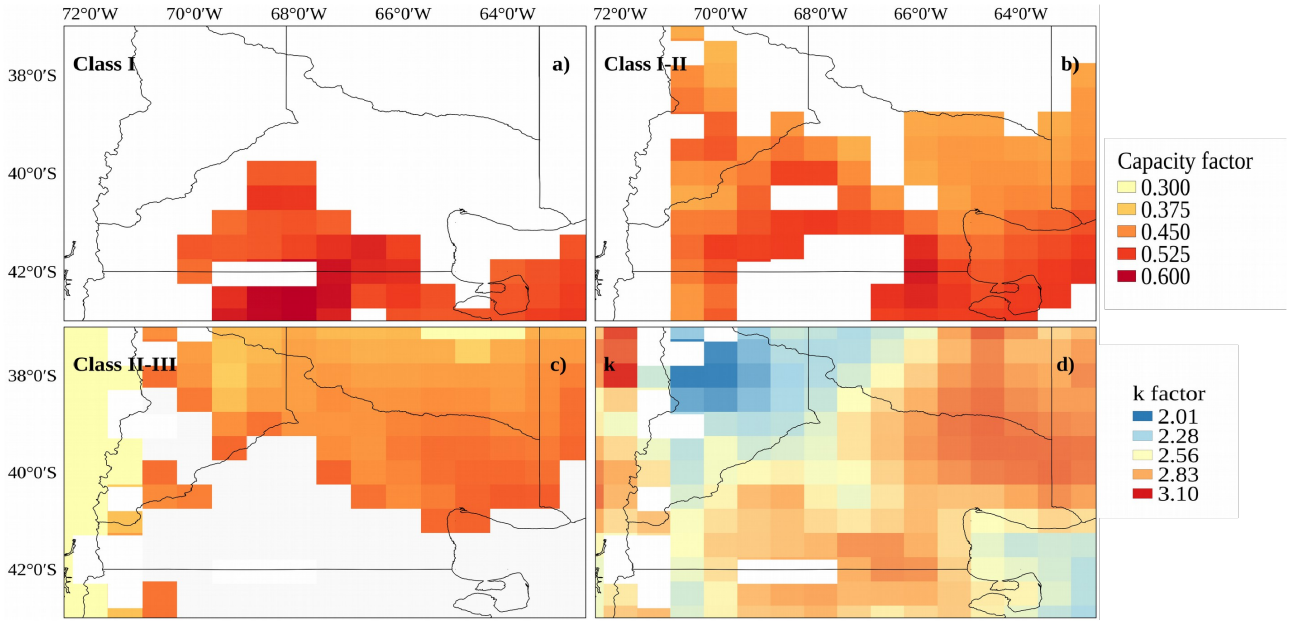

Figure 11: Capacity factors for class I power curve (a), class I and II power curve (b) and class II and III power curve (c). Capacty factors were masked according to its corresponding wind speed range (Table II). k factor of the Weibull distribution (d). Terrain elevations above 1400 masl. were masked.

Tables

Table I: Source, location, percentage of available data and mean wind speed of weather stations, maximum correlation coefficients (r) between wind speed observed at weather stations and wind speed derived from MERRA; and distance between stations and maximum correlation grid point (a). bias, MAE and RMSE statistics (b)

a)

Station	Source	Lat	Lon	Height (m.a.s.l)	Sampling frequency (min)	% Available data	Wind speed (m/s)	Wind speed MERRA (m/s)	r (MERRA vs station)	r distance (km)
Bariloche	SMN	41° 09´ S	71° 10´W	840	60	99,9	5,41	5,20	0,59	155
Maquinchao	SMN	41° 15´ S	68° 44´W	880	180	90	4,17	6,12	0,63	28
San Antonio	SMN	40° 47´ S	65° 06´W	15	60	60	6,26	5,10	0,53	37
Belisle	INTA	39° 12´ S	65° 54´W	128	10	84	1,24	3,86	0,57	78
Cinco Saltos	INTA	38° 50´ S	68° 04´W	282	10	99	0,65	3,81	0,48	55
Guerrico	INTA	39° 01´ S	67° 40´W	242	10	99,9	1,30	3,83	0,54	86
Picun Leufú	INTA	39° 32´ S	69° 18´W	393	10	88	0,34	4,35	0,29	51
Pilcaniyeu	INTA	41° 7´ S	70° 44´W	1010	15	58	2,19	4,07	0,53	14
Villa Regina	INTA	39° 06´ S	67° 06´W	158	10	95	0,88	3,82	0,45	79
Catriel	DPA	37° 51´ S	67° 50´W	320	1440	65	0,57	3,62	0,45	22
Río Colorado	DPA	38° 59´ S	64° 48´W	100	1440	92	3,43	3,63	0,62	12
Sierra Colorada	DPA	40° 35´ S	67° 45´W	660	1440	98	2,63	4,69	0,86	68
Valcheta	DPA	40° 40´ S	66° 10´W	180	1440	75	0,27	3,81	0,25	531
Viedma	DPA	40° 48´ S	63° 00´W	40	1440	92	1,48	4,12	0,65	91

b)

Parameter	value (m/s)
Bias	1,80
MAE	2,34
MSE	2,56

Table II. International Electrotechnical Commission (IEC) wind turbine generator classes

Wind Class/Turbulence	Annual average wind speed at hub height (m/s)	Extreme 50-year gust (m/s)
Ia High wind - Higher Turbulence 18%	10.0	70
Ia High wind – Lower Turbulence 18%	10.0	70
IIa Medium wind - Higher Turbulence 18%	8.5	59.5
IIb Medium wind - Lower Turbulence 16%	8.5	59.5
IIIa Low wind - Higher Turbulence 18%	7.5	52.5
IIIb Low wind - Lower Turbulence 16%	7.5	52.5
IV	6.0	42.0